Power Electronics Laboratory Report
Session 5: Combined AC/DC + DC/DC Converters

Zbigniew Michalak

May 5, 2025

Objectives

- Study the operation of both AC/DC and DC/DC converters.
- Introduction to a simple residential Battery Energy Storage System (BESS).
- Improving grid current quality with an LCL filter.

1 Introduction

This laboratory session investigates a residential Battery Energy Storage System (BESS), designed to supply loads during grid blackouts. The system comprises interconnected DC/DC and DC/AC converters linking a battery storage unit to the grid and local loads, via a common DC-Link. In grid-connected mode, the DC/AC converter typically regulates the DC-Link voltage, while the DC/DC converter manages battery charging and discharging, often optimizing for energy cost by charging during low-price periods and discharging during high-price periods. During blackouts (island mode), the control strategy shifts: the DC/DC converter regulates the DC-Link voltage from the battery, and the DC/AC converter generates the necessary AC voltage for the loads. This experiment focuses solely on the grid-connected mode of operation.

2 Part 1: Grid-Connected BESS Operation

This section details the implementation and testing of the BESS operating in grid-connected mode. The circuit configuration is shown in Figure 1. The AC/DC converter operates as a rectifier to regulate the DC-Link voltage, while the DC/DC converter controls the battery current. The system parameters are provided in Table 1.

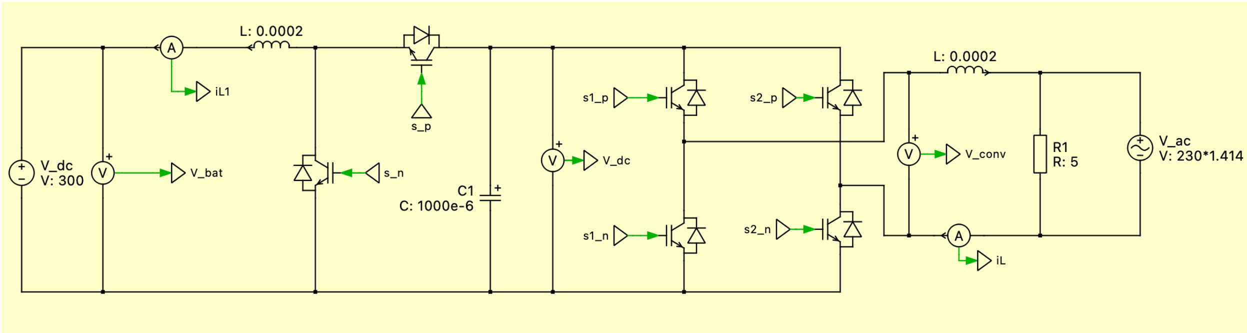

Figure 1: BESS in grid-connected mode configuration.

Table 1: Circuit Parameters.

Parameter	Value
Grid voltage (rms)	230V
DC-Link voltage (nominal)	400V
Nominal battery voltage	300V
Inductance, L (both converters)	200μH
DC-Link capacitance	1000μF
Switching frequency	10kHz
Load resistance	5Ω

2.1 Task 0: System Implementation

The combined AC/DC and DC/DC converter system shown in Figure 1 was implemented in PLECS using the parameters from Table 1. The AC/DC converter uses the control scheme from Session 4 for DC-Link voltage regulation with unipolar modulation. The DC/DC converter employs the current control scheme from Session 2, configured appropriately for the battery voltage (300V) being lower than the DC-Link voltage (400V). The initial DC-Link voltage was set to 400V.

2.2 Task 1: AC/DC Converter Standalone Test (Rectifier Mode)

Before testing the full interconnected system, the operation of the AC/DC converter in rectifier mode was verified independently. The AC/DC converter (Grid source, filter inductor, H-bridge, DC-Link capacitor) was simulated standalone, disconnected from the DC/DC converter section. A constant DC load was applied to the DC-Link capacitor by connecting a Controlled Current Source set to draw 10A. The DC-Link voltage controller (from Session 4) was active with a reference of 400V. The initial DC-Link voltage was set to 0V to observe the controller charging the capacitor and regulating the voltage under load.

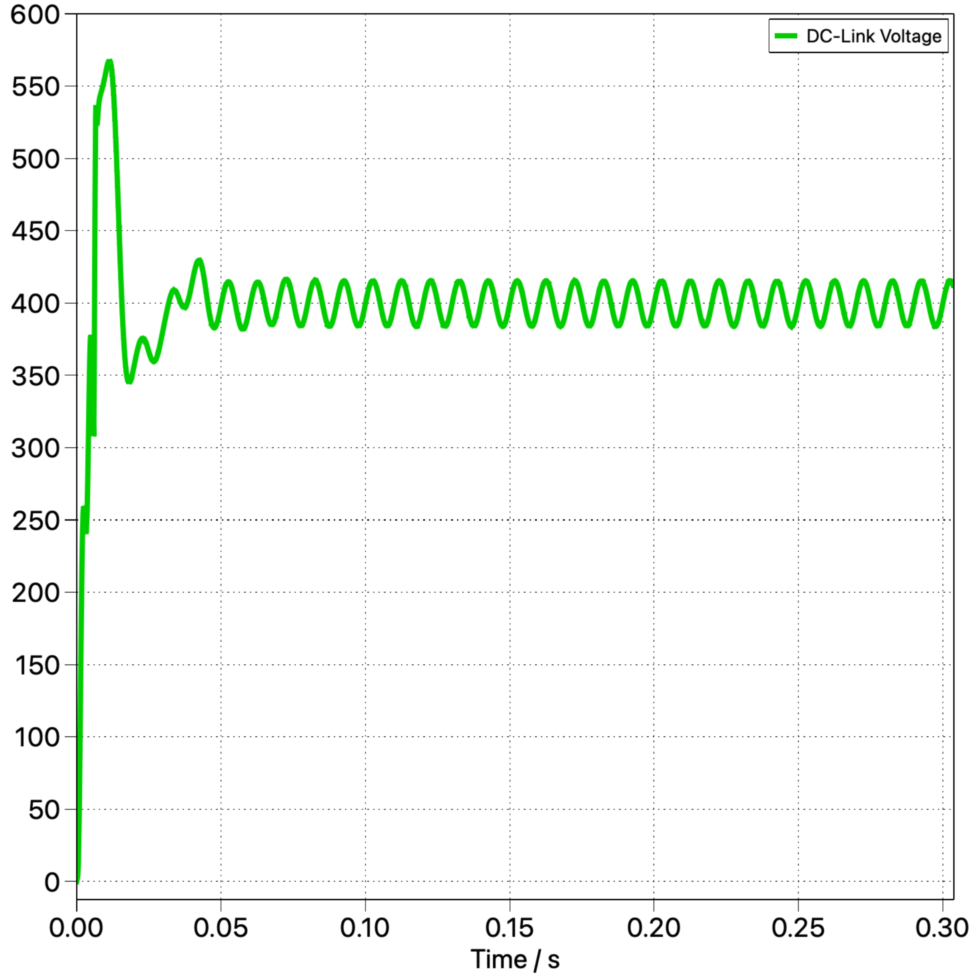

Figure 2: DC-Link voltage (V_{dc}) response during standalone AC/DC rectifier test with a constant DC load.

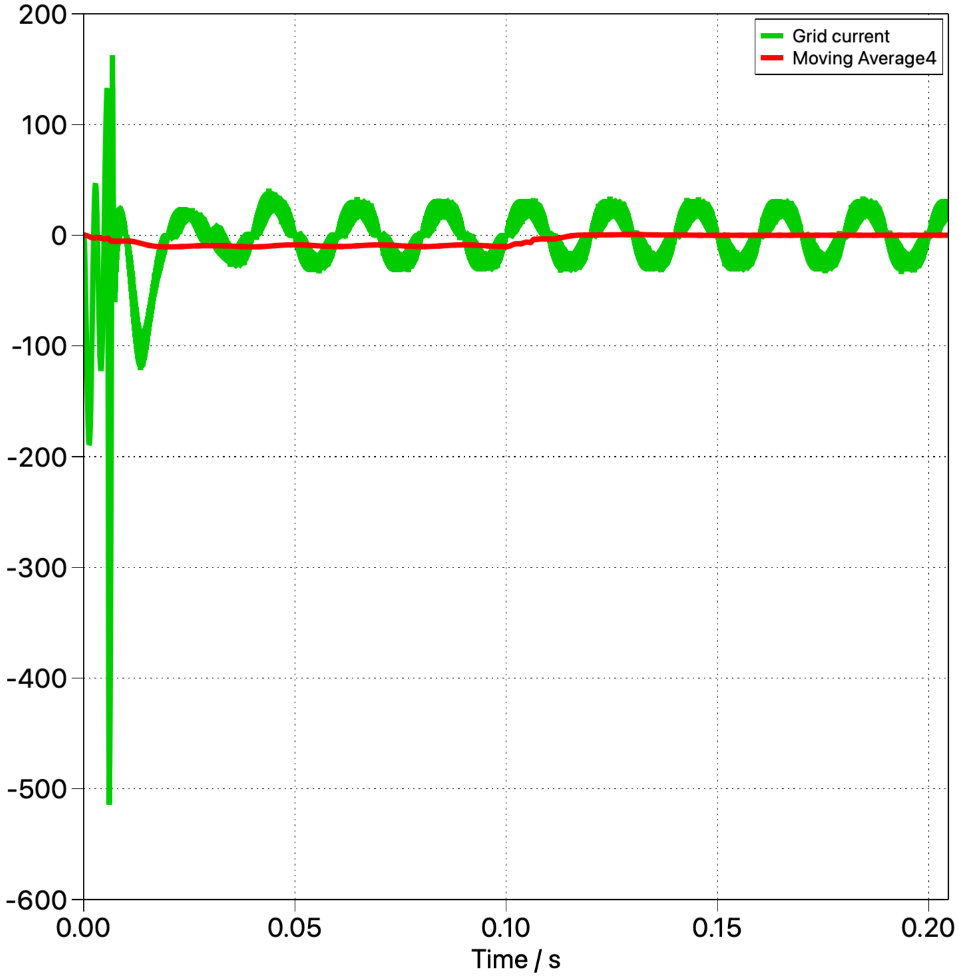

Figure 3: Grid current (I_{grid}) drawn by the AC/DC converter during the standalone rectifier test with a constant DC load.

Observations: Figure 2 shows the DC-Link voltage during the test. The voltage successfully rises from its initial condition and stabilizes accurately around the 400V reference, demonstrating effective voltage regulation by the controller even while supplying the DC load. Figure 3 displays the corresponding grid current drawn from the AC source. The waveform is generally sinusoidal, indicating that the converter is drawing active power from the grid to supply the DC load and cover internal losses, thus confirming correct operation in rectifier mode.

2.3 Task 2: DC/DC Converter Standalone Test

The operation of the DC/DC converter in current control mode was verified independently before interconnecting the full system. For this test, the DC/DC converter section (Battery source, inductor, switching leg, current controller) was isolated. The connection to the main DC-Link capacitor was replaced with an ideal DC Voltage Source set to 400V. A step change was applied to the battery current reference ($I_{bat,ref}$) (from 0A to 10A at t=0.05s) to evaluate the controller's dynamic response and tracking capability.

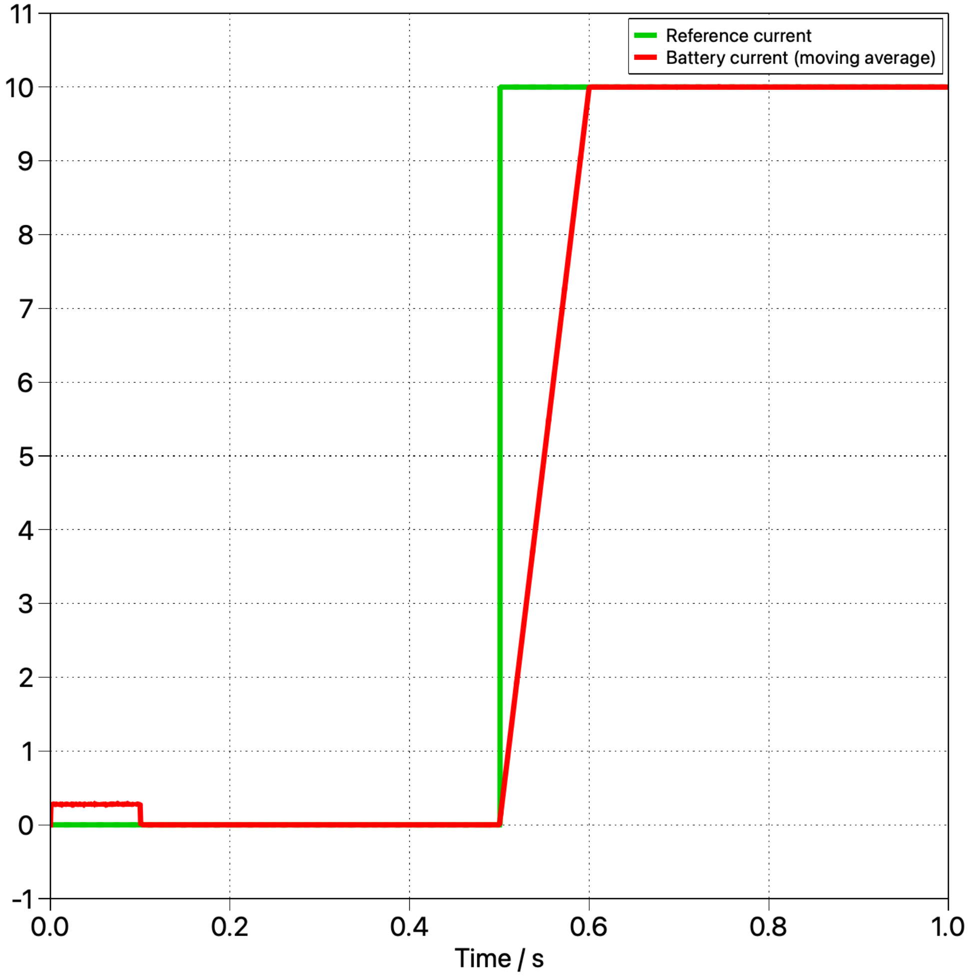

Figure 4: DC/DC converter current control standalone test: Battery current reference ($I_{bat,ref}$) vs. actual measured battery current (I_{bat}) showing response to a step change.

Observations: Simulation results are shown in Figure 4. The plot confirms that the DC/DC converter's current controller successfully tracks the reference current. Following the step change in $I_{bat,ref}$, the measured I_{bat} responds quickly and accurately settles at the new reference value. The response shows good stability with minimal overshoot or oscillation, indicating that the current controller parameters (from Session 2) are appropriate for this converter.

2.4 Task 3: Interconnected System (Zero Battery Current)

The AC/DC and DC/DC converters were interconnected as shown in the full system diagram (Figure 1), with both controllers active. The AC/DC converter's controller was set to regulate the DC-Link voltage (V_{dc}) at 400V, and the DC/DC converter's current controller reference ($I_{bat,ref}$) was set to 0A. The AC load was kept disconnected for this test. The initial DC-Link voltage was set to 400V. The simulation was run to observe the system's steady-state behavior under these idle conditions.

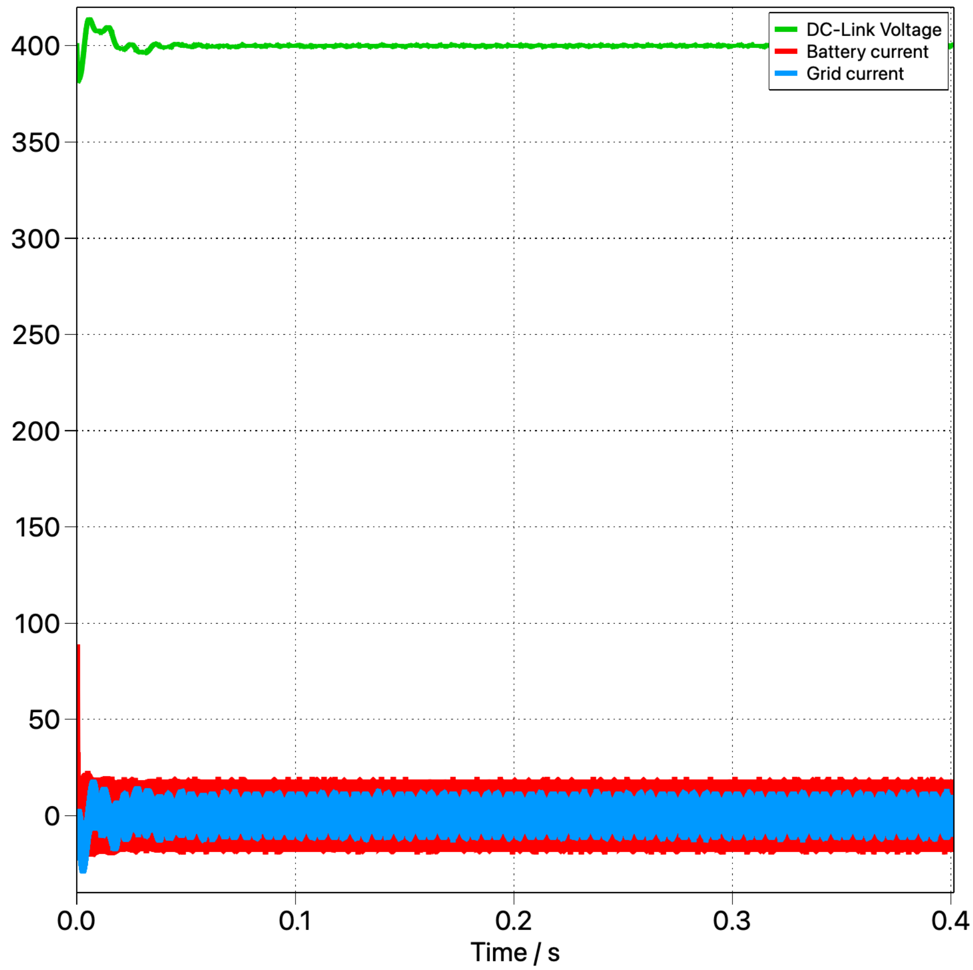

Figure 5: System steady-state waveforms with interconnected converters: DC-Link voltage (V_{dc}), Battery current (I_{bat}), and Grid current (I_{grid}) with $I_{bat,ref} = 0$A and no AC load connected.

Observations: As shown in Figure 5, the interconnected system demonstrates stable operation under idle conditions. The DC-Link voltage (V_{dc}) is successfully regulated and maintained very close to the 400V reference by the AC/DC converter's controller. The battery current (I_{bat}) is effectively controlled to be approximately 0A, following its reference value, but with noticible ripple. The grid current (I_{grid}) shows a small amplitude AC waveform with ripple, indicating that the AC/DC converter draws only the minimal active power required from the grid to compensate for converter switching and conduction losses while maintaining the DC-Link voltage.

2.5 Task 4: Battery Charge and Discharge

The system was simulated to emulate battery charging followed by discharging. The initial battery current reference ($I_{bat,ref}$) was set to +20A, representing charging. However, the simulation starts with $I_{bat} = 0A$, and it takes approximately 0.1 seconds for the actual battery current to ramp up and reach the initial +20A reference. At t=0.3s, the reference was stepped to -20A (discharging). The actual battery current then transitioned, reaching the -20A reference around t=0.4s. The AC load remained disconnected throughout.

Power Calculations (Steady State): Assuming the nominal battery voltage $V_{bat} = 300V$:

- Steady State Charging Power ($I_{bat} = +20A$): $P_{bat,charge} = V_{bat} \times I_{bat} = 300\,V \times 20\,A = 6000\,W$. .
- Steady State Discharging Power ($I_{bat} = -20A$): $P_{bat,discharge} = V_{bat} \times I_{bat} = 300V \times (-20A) = -6000\,W$. .

Assuming ideal lossless converters, the grid active power (P_{grid}) is approximately the negative of the battery power during steady state.

- During Steady State Charging ($I_{bat} = +20A$): $P_{grid,charge} \approx -P_{bat,charge} = -6000W$. Power is drawn from the grid. .
- During Steady State Discharging ($I_{bat} = -20A$): $P_{grid,discharge} \approx -P_{bat,discharge} = -(-6000W) = 6000W$. Power is injected into the grid. .

The steady-state simulation results are expected to align with these calculations.

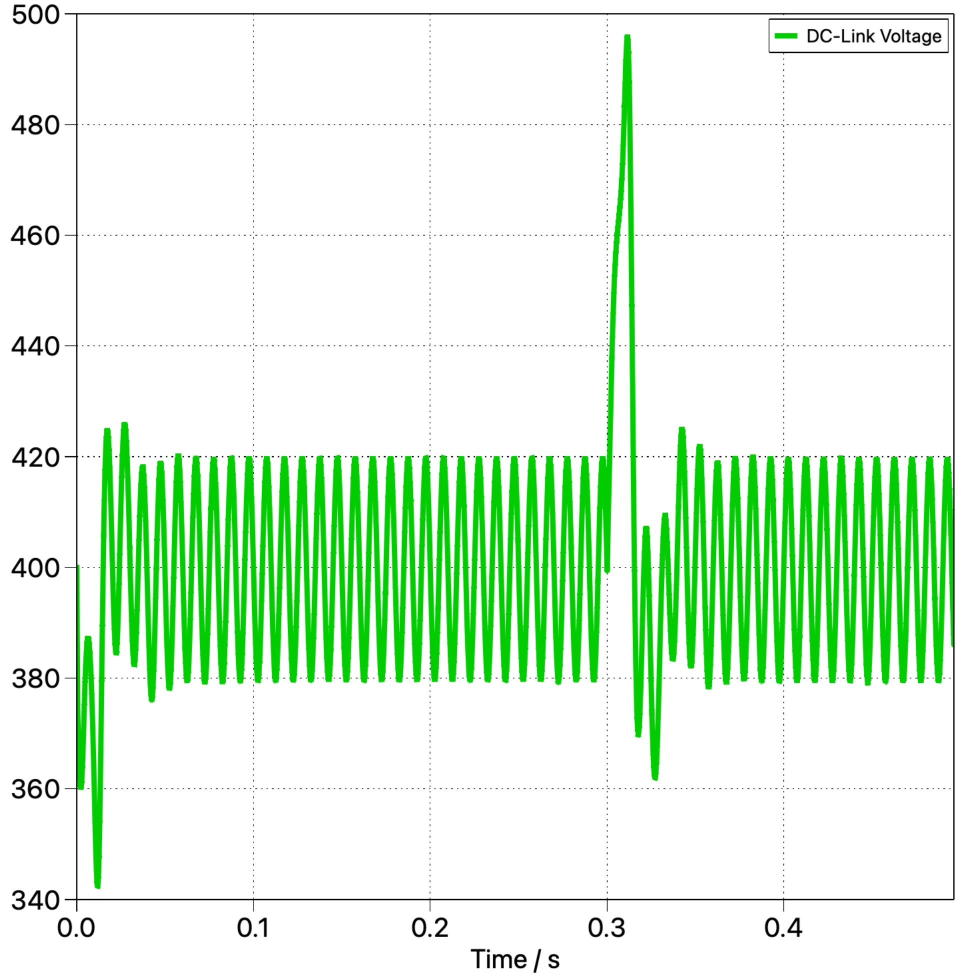

Figure 6: DC-Link voltage (V_{dc}) during the charge/discharge sequence (Initial ramp to +20A, step to -20A at 0.3s).

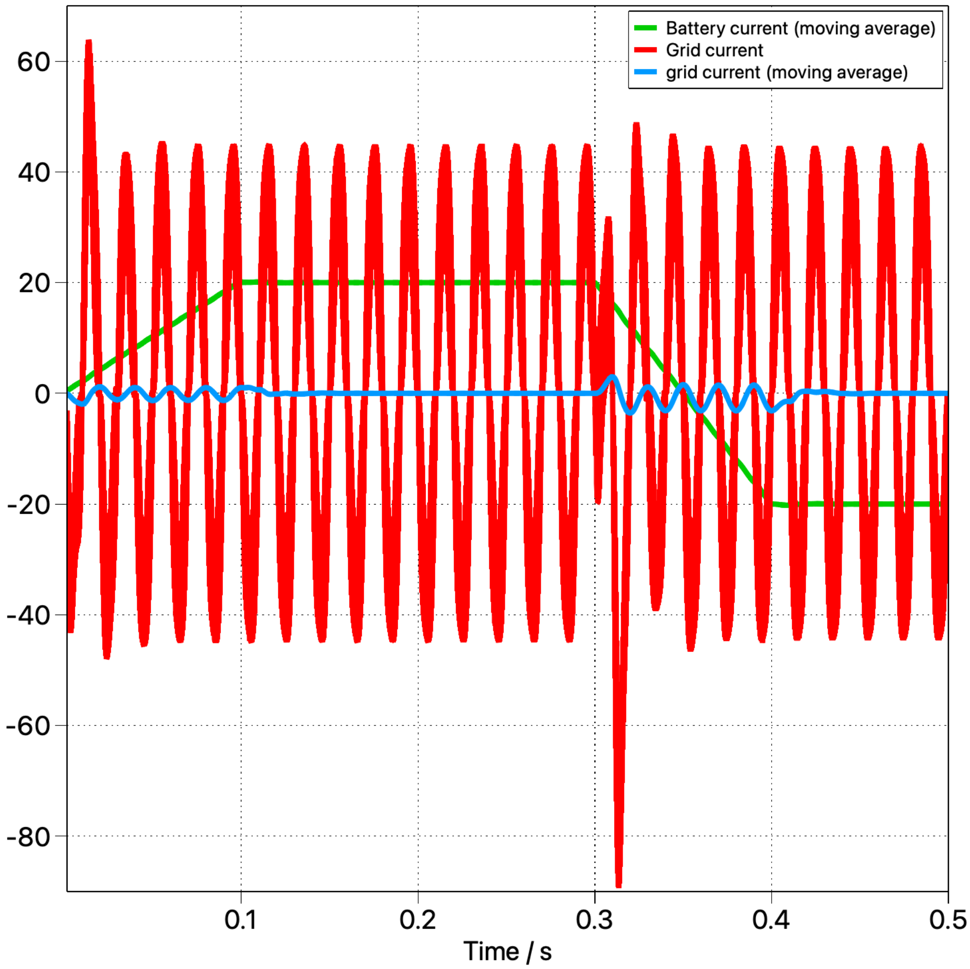

Figure 7: Battery current (I_{bat}) and Grid current (I_{grid}) showing initial ramp (0s-0.1s), steady charge (+20A, 0.1s-0.3s), transition ramp (0.3s-0.4s), and steady discharge (-20A, 0.4s).

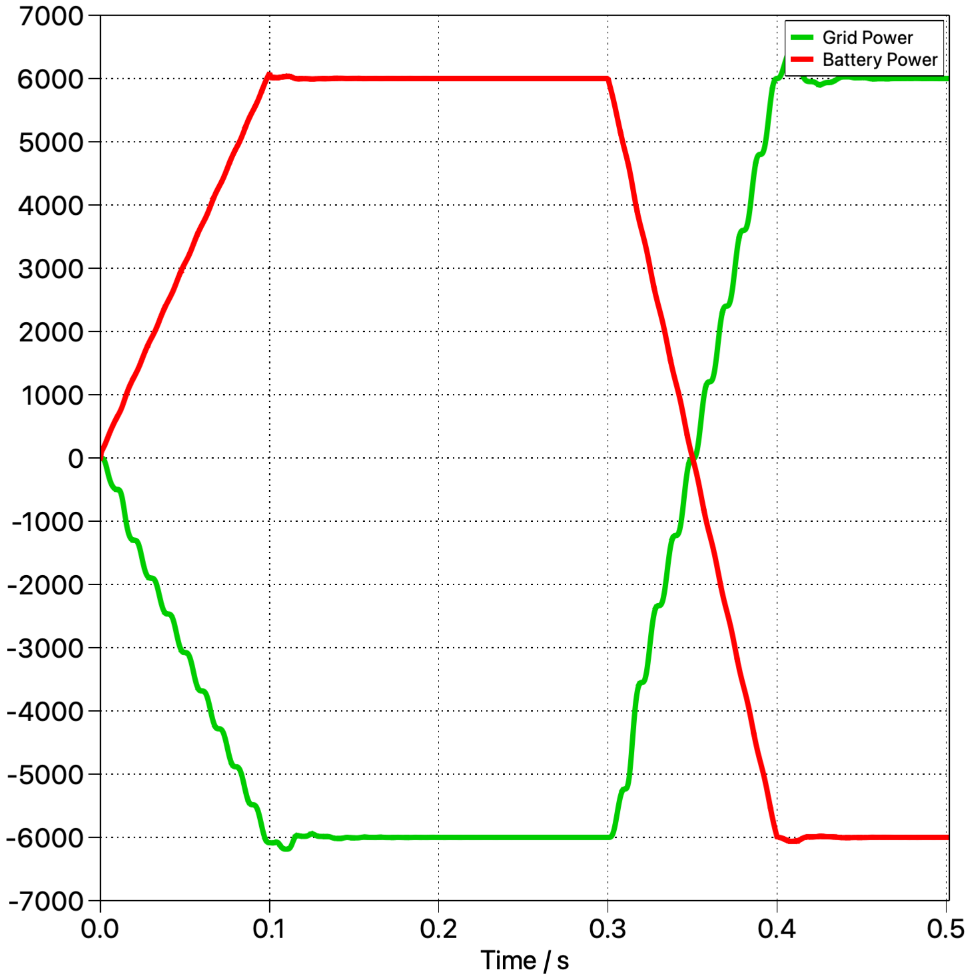

Figure 8: Battery power (P_{bat}) and Grid active power (P_{grid}) corresponding to the current transitions and steady states.

Observations: Figure 6 confirms the DC-Link voltage stability around 400V, maintained by the AC/DC converter's controller throughout the initial current ramp-up and the subsequent transition between charging and discharging. Figure 7 clearly shows the dynamics: I_{bat} ramps from 0A towards the initial +20A reference between t=0s and t=0.1s. It remains steady at +20A between t=0.1s and t=0.3s (steady charging). At t=0.3s, the reference changes to -20A, and I_{bat} ramps down, reaching -20A around t=0.4s. After t=0.4s, it stays at -20A (steady discharging). The grid current I_{grid} waveform changes accordingly, showing significant power draw from the grid during the steady charging phase (0.1s-0.3s) and significant power injection into the grid during the steady discharging phase (after 0.4s), with transient behaviour during the ramps. Figure 8 illustrates the corresponding power flows. P_{bat} ramps up initially, settles near +6000W during steady charging, transitions through zero around t=0.35s (mid-ramp), and settles near -6000W during steady discharging. P_{grid} shows the opposite behaviour, settling near -6000W (power draw) during steady charging and near +6000W (power injection) during steady discharging, aligning with steady-state calculations. .

2.6 Task 5: Supplying Load from Battery

The objective is to supply the connected load ($R_{load} = 5\Omega$) primarily from the battery, minimizing active power drawn from the grid.

Calculations
Nominal AC Load Power: $P_{load} = V_{g,rms}^2/R_{load} = (230\,\mathrm{V})^2/5\,\Omega = 52900/5 = 10580\,\mathrm{W}$.
Required Power from DC-Link (assuming ideal AC/DC converter): $P_{dc\_link} \approx P_{load} = 10580\,\mathrm{W}$.
Required Battery Power (assuming ideal DC/DC converter): $P_{bat,req} \approx P_{dc\_link} = 10580\,\mathrm{W}$.
Required Battery Current Magnitude: $|I_{bat,req}| = P_{bat,req}/V_{bat} = 10580\,\mathrm{W}/300\,\mathrm{V} \approx 35.27\,\mathrm{A}$.
Required Battery Current Reference: $I_{bat,ref} = -35.27\,\mathrm{A}$.

Simulation Sequence: The system was simulated following the sequence: (1) Load disconnected, $I_{bat} = 0$. (2) Connect load ($R_{load} = 5\Omega$) at $t = t_1$. (3) Wait for steady state. (4) Apply calculated $I_{bat,ref} \approx -35.27\,\mathrm{A}$ at $t = t_2$. The results are shown in Figure 9.

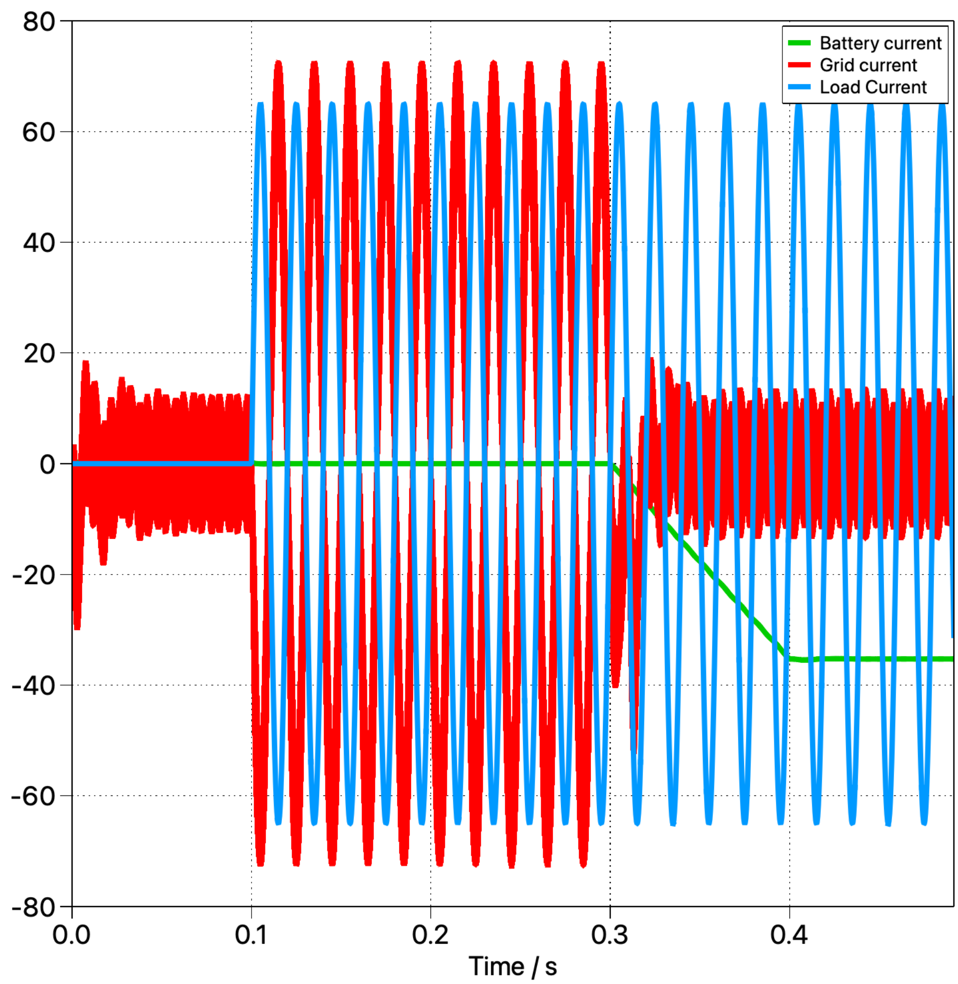

Figure 9: System response during load connection (t_1=0.1s) and battery supply (t_2=0.3s) sequence (I_{bat}, I_{grid}, I_{load}).

Observations: When the load is connected, the grid current I_{grid} increases significantly. When the battery current command ($I_{bat,ref}$) is applied, I_{bat} ramps down to the reference value (approx. -100.6A). Grid current goes to zero.

2.7 Task 6: Grid Current Quality Improvement with LCL Filter

To improve the grid current waveform quality, the inductor filter (L) of the AC/DC converter was replaced with an LCL filter ($L_1 = L_2 = 200\mu H$, $C = 10\mu F$), as shown in Figure 10. The controller still measures the converter-side current (i_{L1}). The system was simulated again (e.g., under load supply condition from Task 5) to compare the grid current (I_g) harmonic content with the original L filter (Figure 11) and the LCL filter (Figure 13).

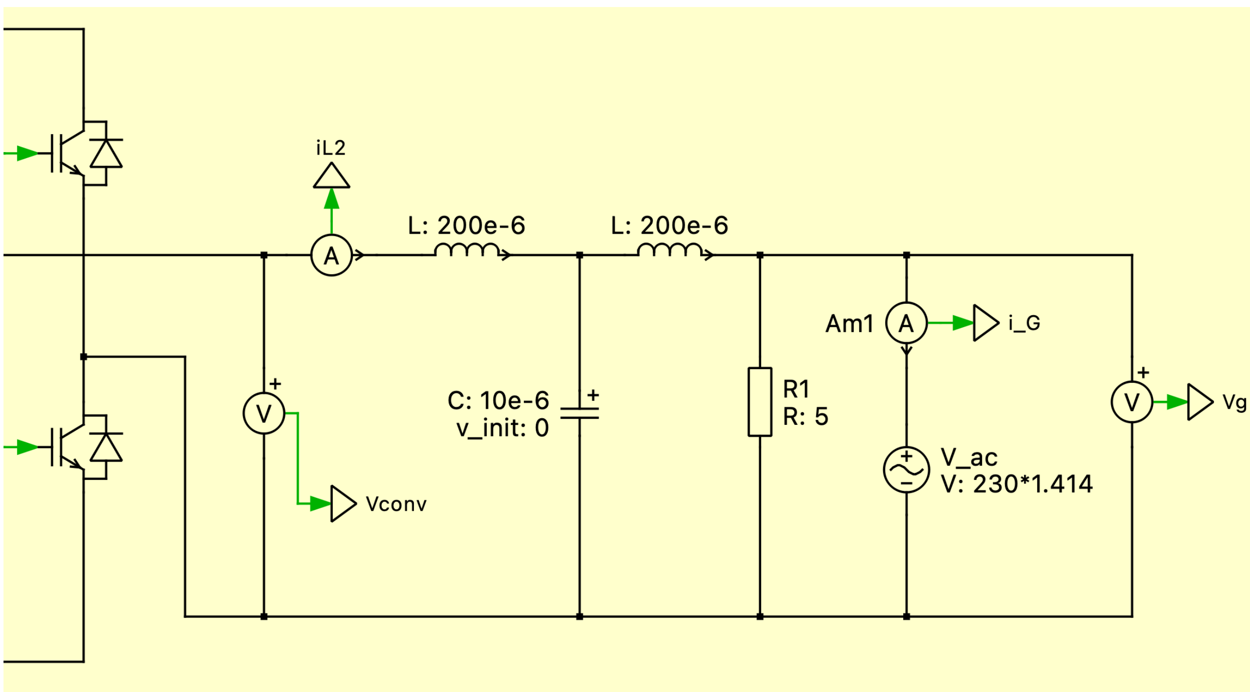

Figure 10: AC/DC converter with LCL filter configuration.

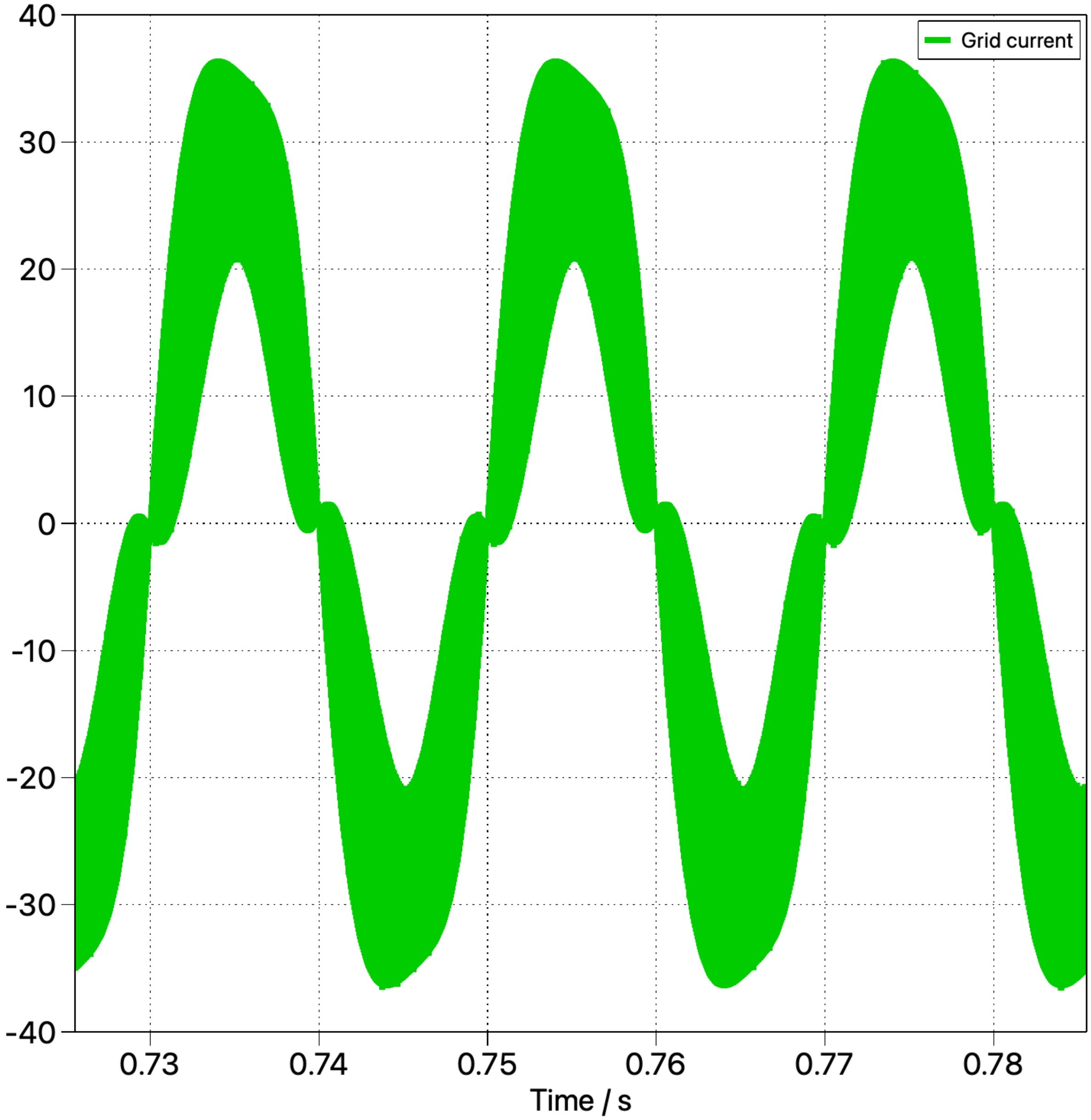

Figure 11: Grid current (I_g) waveform with the original L filter.

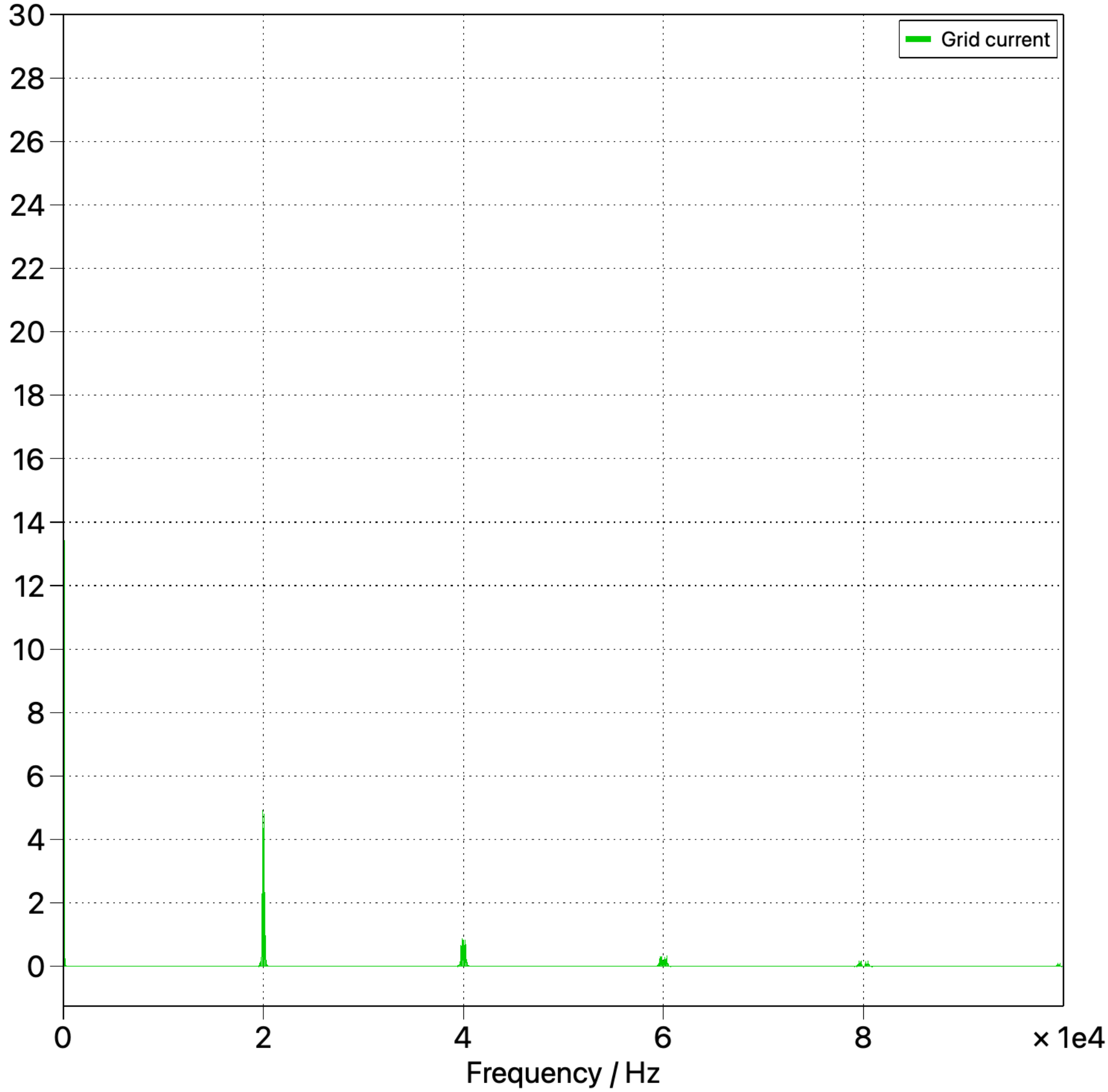

Figure 12: Grid current (I_g) FFT with the original L filter. Multiple harmonics clearly visible.

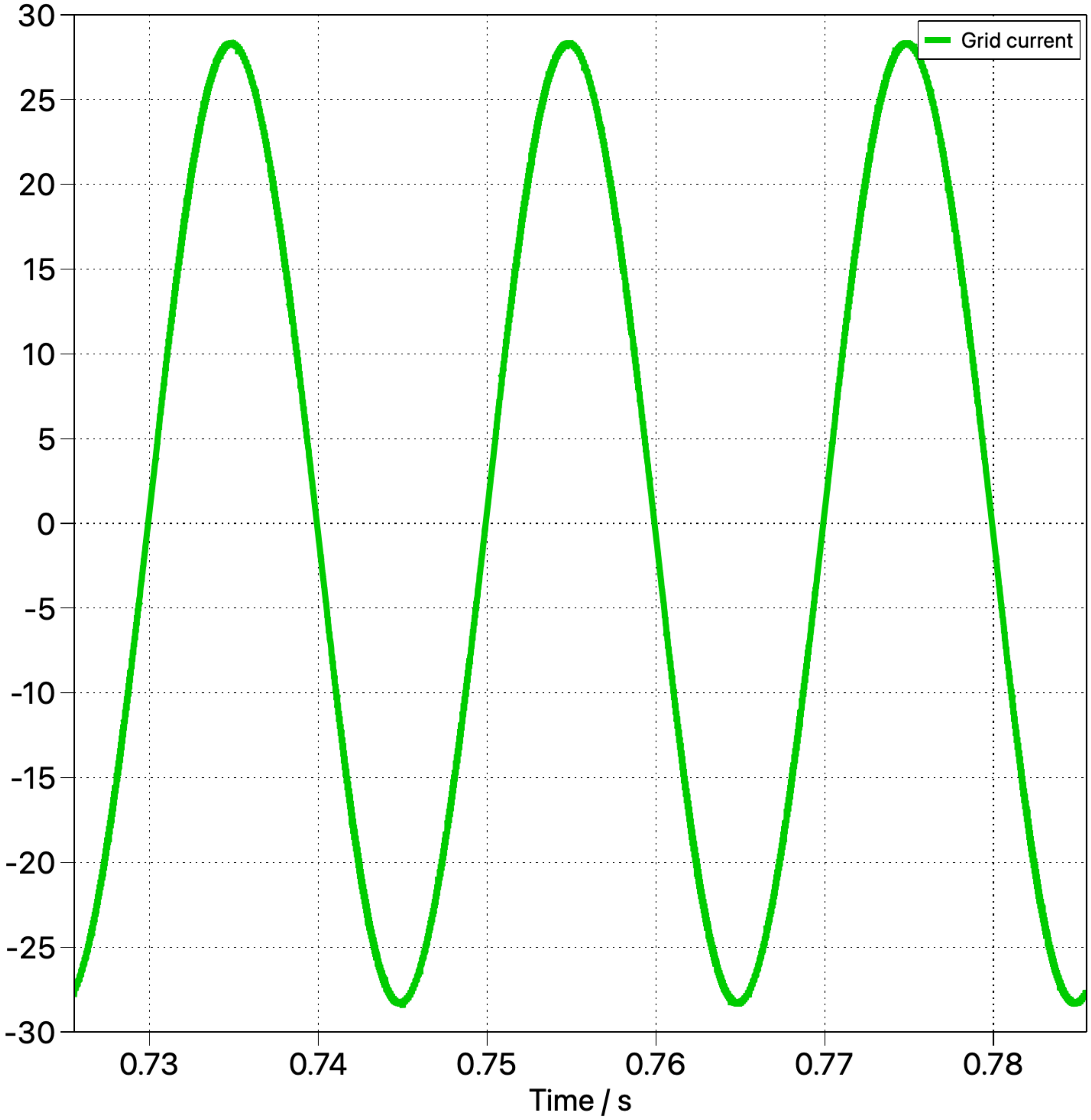

Figure 13: Grid current (I_g) waveform with the LCL filter.

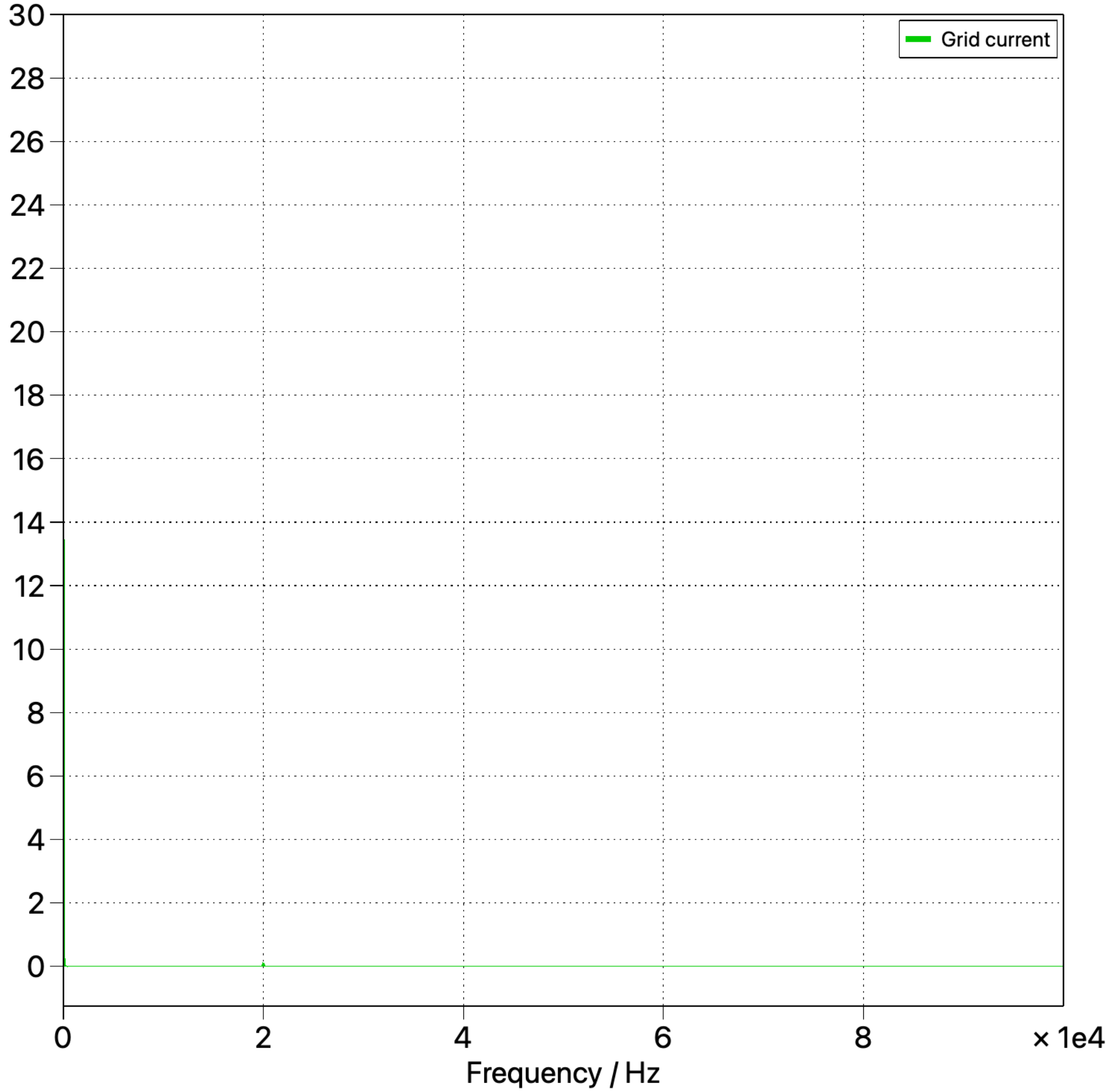

Figure 14: Grid current (I_g) FFT with LCL filter. Significant reduction of harmonics.

Observations: Comparing Figure 13 with Figure 11, the grid current waveform with the LCL filter is significantly smoother and closer to a pure sinusoid, indicating a substantial reduction in high-frequency harmonics compared to the L filter case.

Conclusion

This session demonstrated the grid-connected operation of a BESS model incorporating coupled AC/DC and DC/DC converters. The implementation allowed for the verification of independent control functions: DC-Link voltage regulation by the grid-tied AC/DC converter and battery current control via the DC/DC converter. Bidirectional power flow was achieved, enabling simulation of battery charging from the grid and discharging to the grid, with calculated power levels matching the simulation results. The system was capable of supplying a local DC load primarily from the battery, significantly reducing the power drawn from the AC grid, as confirmed by the calculated required battery current and simulation results. Finally, the effectiveness of using an LCL filter over a simple L filter in attenuating switching harmonics and improving the quality of the grid current was clearly observed. The experiments provided practical insights into the control and operational characteristics of BESS in grid-connected mode.